ANALYSIS OF FINISHING VERY PRECISE HOLES BY THE REAMING HEAD MT3

JOSEF SEDLAK[1], KAREL KOURIL[1], JOSEF CHLADIL[1], ALES JAROS[1], STANISLAV FIALA[2], ZDENEK FIALA[3],

[1]Brno, University of Technology, Faculty of Mechanical Engineering, Institute of Manufacturing Technology, Brno, Czech Republic

[2]Brno, FINAL Tools Inc., Brno, Czech Republic

[3]Kurim, Intemac Solutions Ltd., Kurim, Czech Republic

DOI : 10.17973/MMSJ.2018_10_2017101

e-mail: sedlak@fme.vutbr.cz

The paper deals with the analysis of the finishing of very precise holes by the applied MT3 reaming head from FINAL Tools Inc. In the case of a narrow range of customers with particularly high demands on the quality of the holes is currently appearing effort to elaborate a detailed evaluation of surface quality through evaluation of surface integrity.
These facts led to the design of an experimental part in the form of an analysis of the surface integrity of the test holes machined by the reaming head MT3 during its durability. Surface integrity was assessed from the point of view of circularity, cylindricality, surface roughness, surface defects controlled by electron microscopy, microhardness and metallographic analysis of lateral extrusion. For the completeness of the measured parameters, the dimension of the reamed test holes was also measured.

KEYWORDS

MT3, reaming heads, finishing operations, precise holes, surface integrity

1 INTRODUCTION

The main factors that today accelerate the development of cutting tools are in particular the ever-increasing demands for increasing efficiency and productivity of production, while reducing operating costs, application of difficult materials, environmental issues, health and growing demands for greater safety [Forejt 2006] [Piska 2010] [Slany 2013] [Zouhar 2009].
Reaming head MT3, see Fig. 1 is a productive tool for finishing very precise holes. The head is thermally clamped into the tool body. Heat clamping ensures reliable and accurate setting of the reaming head without adjustment. Easy replacement of the head of the tool body is comparable to an indexable insert in the tool holder, which also brings the same benefits - speed, ease and accuracy of the cutting tool replacement [Forejt 2006] [Piska 2010] [Slany 2013] [Zouhar 2009].

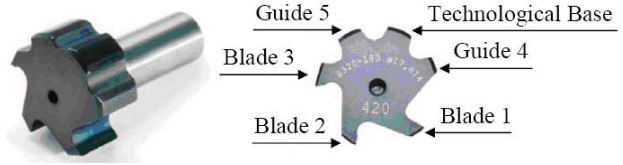

Figure 1. Reaming head MT3

2 EXPERIMENTAL RESEARCH - SURFACE INTEGRITY EVALUATION OF MACHINED TEST HOLES

The main impetus for the implementation of the experimental part was the effort of the Final Tools Inc. employees to learn in detail, how their new design solution of the MT3 reaming head will affect the machined surface of the holes [Havlik 2012].

2.1 Experiment design

For the experiment, the MT3 reaming head of the existing construction with cermet uncoated blades and polycrystalline diamond guides from FINAL Tools Inc. was selected. Three reaming heads MT3 (one at the beginning, one at the center and one at the end of its durability) were used to capture the effect of this cutting tool on the machined surface. One new MT3 reaming head, one reaming head MT3, which had the production of 100 pcs of hydro motors in Sauer Danfoss, which corresponds to the durability from the point of view of the recessed opening L_T = 59,000 mm, was chosen. The last reaming head of the MT3 had a production of 200 hydraulic motors, which corresponds to the durability from the view of the length of the recessed opening L_T = 118,000 mm. The value of 200 hydraulic motors is limited by Sauer Danfoss for the use of one MT3 reaming head in order to maintain safety against the production of scrap parts (the MT3 reaming head is then automatically removed and goes to the manufacturer for renovation). The reaming head MT3 may also be discarded earlier, for example, due to non-compliance with the required surface roughness. With each of the three cutting tools, two test holes (samples) were machined under the same operating conditions into the same material as the cylinders of the hydraulic motors. Subsequently, the surface integrity of these samples was evaluated: circularity, cylindricalness, surface roughness, changes in microhardness, metallographic analysis of the cross-section and evaluation of surface defects under the electron microscope. For the completeness, the dimension of the reamed test holes was also measured [Havlik 2012].

2.2 Semi-finished material

For the experiment, a semi-finished material was selected which is identical to the material used in Sauer Danfoss Hydromotors. This is the 42CrMo4 steel (equivalent to ČSN 15 142) refined to 1000 MPa with chemical composition according to Table 1 and blank sizes of the blank: 200 mm long, 95 mm wide and 27 mm high. The machining of the test holes was carried out on the DECKEL MAHO DMU 60T 5-axis CNC machining center [Bohdan Bolzano, Ltd 2017] [Forejt 2010] [Havlik 2012].

Steel	Chemical composition [weight %]								
	C	Mn	Si	Cr	Ni	Mo	P	S	Fe
15 142 (42CrMo4)	0.38-0.45	0.50-0.80	0.17-0.37	0.90-1.20	max. 0.50	0.15-0.30	max. 0.035	max. 0.035	residue

Table 1. Chemical composition of semifinished material [Bohdan Bolzano, Ltd 2017] [Havlik 2012]

2.3 Applied cutting tools

For the experimental part, the modern reaming head MT3, patented by FINAL Tools Inc., was chosen. The tool has three blades and two guides. The area between the guides serves as the technological base for checking and measuring the reamer diameter. The tolerance field of the holed hole is within the range IT5 to IT6. The surface roughness after the reaming operation reaches values below Ra = 0.3 μm [Fiala 2016] [Kouril 2007].
In Table 2 is a list of all applied tools, including their cutting conditions, used to make test holes. The reaming operation was performed by a reaming head MT3 with non-coated cermet cutting edges and polycrystalline diamond guides. The applied process fluid was RHENUS R-COOL-S emulsion at 10% and 40 bar pressure. For the production of test holes were subsequently used following technological operations, which

are identical to the tool number specified in Table 2 [Havlik 2012] [OE217 – EUREKA] [Sedlak 2011]:

1. Drilling (Centering drill ø1.5x60° DIN 333A HSS),

2. Drilling (drill bit DIN 338 HSS Co ø8 mm),

3. Drilling holes (drill bit SK M44 ø17 mm),

4. Boring (HF boring bar with VBD CCMT 060204 ø17.7 mm +0.05 mm),

5. Reaming (Reamer MT3 ø17.814 mm).

Tool number	Cutting speed v_c [m.min^{-1}]	Feed rate f_{ot} [mm]	Cooling
1.	35	0.05	Yes
2.	35	0.1	
3.	95	0.15	
4.	150	0.35	
5.	200	0.42	Yes

Table 2. Cutting conditions used for individual cutting tools [Havlik 2012] [Sedlak 2011]

According to the Table 2 a total of 6 test holes were made in the blank. For the two test holes, the new (unworn) reaming head MT3 was used in the reaming operation. For the other two test holes, a reaming head MT3 was used which was behind L_T = 59,000 mm of the bore. For the last two test holes, a reaming head MT3 was used which was behind L_T = 118,000 mm of the bore. The test holes were marked as shown in Table 3 [Havlik 2012].

Reaming head MT3	Designation of the test hole
New	MD50
	MD51
Used; L_T = 59,000 mm	W1A
	W1B
Used; L_T = 118,000 mm	W2A
	W2B

Table 3. Designation of test holes [Havlik 2012]

2.3.1 Machining before reaming

As described in the article, hole machining technology has been divided into 5 steps: drilling, drilling (8 mm and 17 mm diameter) followed by boring with boring bar and reaming.

The key element to achieve the very high dimensional and shape precision and quality of the machined hole is the hole condition before reaming. In view of the above, boring bar has been included in the drilling technology for testing. It is a single-blade tool with cutting insert of sintered carbide of its own construction by FINAL Tools Inc. The shank of the boring bar is made of sintered carbide and only the bed for the cutting insert is steel. The process fluid is brought to the cutting insert edge directly by the shank. The sintered carbide shank ensures high rigidity, high precision. If there is no other adverse effect such as machine spindle inaccuracy, stiffness of clamping, etc., the single-blade rigid tool "describes" machining, an almost ideal spiral. This is complemented by a suitably chosen cutting insert with positive geometry and a small radius of blade. The result is a hole with very good shape and dimensional precision, ready for the final reaming operation. Practical tests have proved that without boring bar mentioned structure, it is possible to repeatedly achieve the desired results. After drilling, the addition of approximately 0.15 mm will remain for reaming. Reaming, including the use of MT3, can only very slightly improve the shape accuracy (especially cylindricality) of machined holes. The reaming head MT3 subsequently produces a very productive quality of the work surface and, due to its 3-blade design and 2 guides, ensures the characteristic surface integrity.

2.4 Evaluation of test holes - measurement of dimension, circularity and cylindricality

Measurement of three sets of test specimens, each with two reamed test holes, was carried out on the Carl Zeiss PRISMO 7 three-coordinate measuring instrument, which allows measurement of circularity and cylindricality in discontinuous and continuous mode [Havlik 2012].

Measuring the dimensions of test holes were performed by a continuous mode (scanning method) with the number of 18 dots per 1 mm. The circularity was measured at 4 levels of the test hole, 4 longitudinal sections were added in the direction of the axis of the opening by 90 ° of the perimeter of the opening, see Fig. 2. From the measured values the instrument determined the diameter and the cylindricalness of the test hole [Fiala 2015] [Havlik 2012] [Kouril 2006].

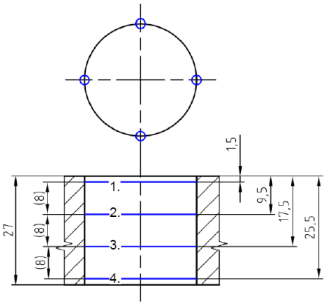

Figure 2. Circularity and cylindricality measurement of the test hole [Havlik 2012]

In Table 4 the measured values of the hole dimensions, the circularity in 4 levels of the holes lengths are shown, see Fig. 2 - the average value of these 4 circularities and the hole cylinders [Havlik 2012].

Hole	Size [mm]	Circl. 1. [mm]	Circl. 2. [mm]	Circl. 3. [mm]	Circl. 4. [mm]	Circl. averege [mm]	Cylindr. [mm]
MD50	17.8203	0.0043	0.0030	0.0028	0.0029	0.0033	0.0060
MD51	17.8209	0.0044	0.0027	0.0031	0.0026	0.0032	0.0061
W1A	17.8118	0.0067	0.0045	0.0028	0.0031	0.0043	0.0089
W1B	17.8104	0.0062	0.0042	0.0034	0.0037	0.0044	0.0083
W2A	17.8100	0.0057	0.0039	0.0020	0.0032	0.0037	0.0081
W2B	17.8114	0.0051	0.0038	0.0024	0.0025	0.0035	0.0066

Table 4: Measured values for the size, circularity and cylindricality of the test holes [Havlik 2012]

From the measured values see Table 4 it follows that the size of the test holes ranged from 17.8100 mm to 17.8209 mm, the average hole circularity ranged from 0.0032 mm to 0.0044 mm and a cylindrical dimension was in the range of 0.0060 mm to 0.0089 mm. The lowest values of circularity and cylindricality are represented by the MD50 and MD51 test holes made by the new reaming head MT3. When comparing the roundness values in each hole level, all test holes show the largest circularity values at the beginning of the hole. This can be caused by vibrating the tool when it starts cut [Fiala 2015] [Havlik 2012] [Kouril 2006].

2.5 Measurement of surface roughness of the test holes

Surface roughness measurement of test holes was carried out on the measuring instrument Form Talysurf Intra 5.0 Taylor Hobson. The length of the 27 mm test hole was divided into 3 sections of 10 mm in Fig. 3. The roughness measurement was performed in one straight line over the entire length of the test hole. To maintain the same rated length of 10 mm for all sections, the 3rd section was measured at a length of 10 mm from the end of the hole. Measured sections 2 and 3 thus partly overlapped [Fiala 2015] [Havlik 2012] [Kouril 2006].

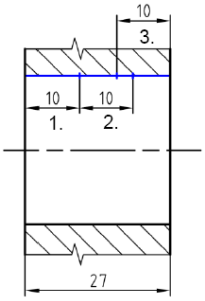

Figure 3. Surface roughness measurement of the test hole [Havlik 2012]

In Table 5, the measured values of the roughness parameters Ra and Rz are given in three sections of the length of the measured test holes, see Fig. 3 and the average values of these three values of the parameters Ra and Rz.

Test hole	Roughness parameter Ra [µm]				Roughness parameter Rz [µm]			
	1.	2.	3.	Average	1.	2.	3.	Average
MD50	0.1823	0.1701	0.1682	0.1735	1.0092	0.9699	0.9750	0.9847
MD51	0.1630	0.1704	0.1757	0.1697	0.9228	0.9671	1.0069	0.9656
W1A	0.1183	0.1172	0.1183	0.1179	0.7072	0.7749	0.7432	0.7418
W1B	0.1288	0.1192	0.1207	0.1229	0.7576	0.7382	0.7674	0.7544
W2A	0.1335	0.1418	0.1457	0.1403	0.8188	0.8733	0.9290	0.8737
W2B	0.1384	0.1637	0.1669	0.1563	0.8184	1.0493	1.0098	0.9592

Table 5. Measured values of roughness parameters Ra and Rz of test hole surface [Havlik 2012]

From the measured values in Table 5 it follows that the average values of surface roughness parameters Ra ranged from 0.1179 µm to 0.1735 µm, the average values of surface roughness parameters Rz ranged from 0.7544 µm to 0.9847 µm. Comparison of the measured values of the Ra and Rz parameters in the individual sections does not show for all test holes a possible increase in surface roughness in the 1st section of the test holes as in the case of a previous roundness evaluation. This trend shows only the MD50 test aperture, with the highest surface roughness at the beginning of the test hole and further decreasing. For the other test holes, the maximum and minimum measured values of roughness alternate gradually across all measured sections. More test holes, including statistical evaluation, would have to be made more precise [Fiala 2015] [Havlik 2012] [Kouril 2006].

2.6 Preparation of test samples

For the following evaluation of microhardness, metallographic evaluation, and evaluation of the machined surface under a scanning electron microscope, the test specimens were taken from the blank with the holes obtained by electro-erosion machining, see Fig. 4 [Fiala 2015] [Havlik 2012] [Kouril 2006].

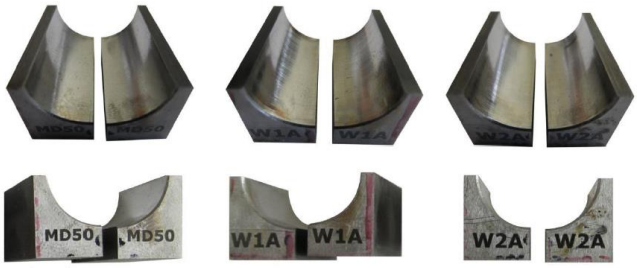

Figure 4. Removed test samples from a blank workpiece [Havlik 2012]

This set of test samples was additionally supplemented with a test sample taken from the cylinder of a hydraulic motor as shown in Fig. 5 manufactured by Sauer Danfoss. This test sample designated MD1h, was made using the same technological procedure as the test samples made in the experiment (drilling, drilling, reaming) but followed by finishing roller operations. This test was used to evaluate the microhardness, metallographic evaluation, and evaluation of the machined surface under a scanning electron microscope to compare the state of the machined surface to a real hydromotor in practice, followed by roller operations after reaming [Havlik 2012] [Pokorny 2012].

Figure 5. Test sample of cylinder of hydraulic motor ; reaming carried out on: 9 x ø17.5 mm, depth 65.48 mm (partially through hole) [Fiala 2015] [Havlik 2012] [Kouril 2006]

2.7 Evaluation of surface defects under an electron microscope

For the evaluation of surface defects on the machined surface of the test samples a scanning electron microscope, Philips XL30 ESEM was used.

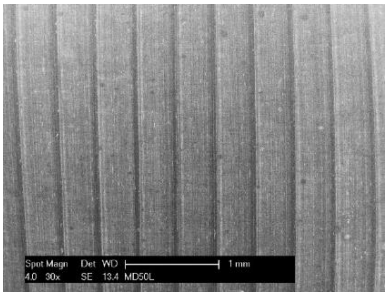

Figure 6. Surface condition of machined test samples; sample MD50 [Havlik 2012]

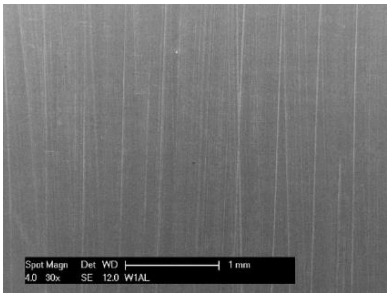

Figure 7. Surface condition of machined test samples; sample W1A [Havlik 2012]

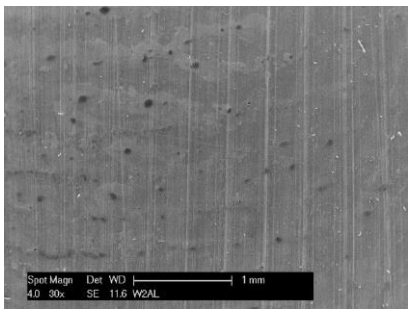

Figure 8. Surface condition of machined test samples; sample W2A [Havlik 2012]

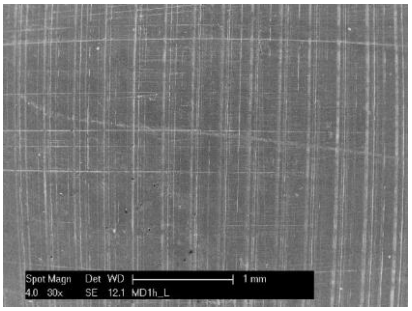

Figure 9. Surface condition of machined test samples; sample MD1h [Havlik 2012]

Already at 30x magnification images are noticeable differences. Regular deep machining tracks are also visible in Fig. 6, which correspond to the highest measured surface roughness values for the MD50 and MD51 test specimens made by the reaming head at the beginning of its life time. Fig. 8 shows a trace of corrosion damage on test sample W2A. Fig. 9 shows the densely deformed traces of machining followed by rolling. More detailed differences in the state of machined surfaces are captured on other frames with greater magnification (the hole axis is horizontal across all frames) [Dugin 2012] [Fiala 2015] [Havlik 2012] [Kouril 2006] [Pokorny 2016].

Fig. 10 shows unconfirmed indications of so called „transgenes“, which were later identified as a local hardened layer on the metallographic cut. The visible traces of the new reamer head MT3 at the beginning of its durability then had a greater depth, resulting in a higher surface roughness [Dugin 2012] [Fiala 2015] [Havlik 2012] [Kouril 2006] [Pokorny 2016].

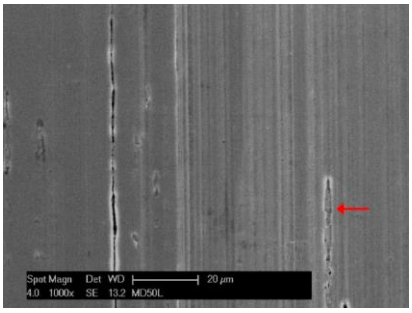

Figure 10. Test sample MD50 (magnification 1000x) [Havlik 2012]

Fig. 11 shows a more smoothed surface with places with deeper traces, which could have been worse leaving the chip. This state of surface after machining with the MT3 reaming head in the middle of its life time also corresponds to the measured lower roughness values compared to the test samples made by the new reaming head MT3 at the beginning of its life time [Dugin 2012] [Fiala 2015] [Havlik 2012] [Kouril 2006] [Pokorny 2016].

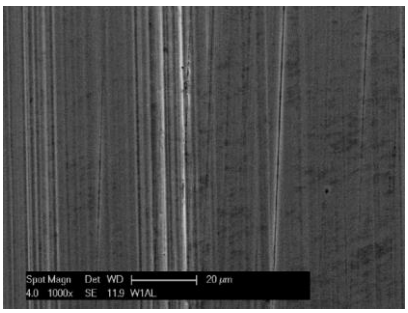

Figure 11. Test sample W1A (magnification 1000x) [Havlik 2012]

Fig. 12 illustrates a similar state of surface after machining with the reaming head MT3 at the end of its life time with the surface condition of the previous case, i.e. the reaming head MT3 in the middle of its durability. Both machined surfaces are visible both as smoothed spots and deeper traces of machining [Dugin 2012] [Fiala 2015] [Havlik 2012] [Kouril 2006] [Pokorny 2016].

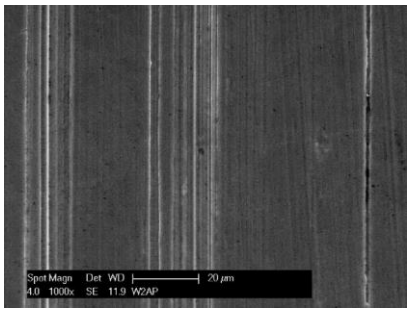

Figure 12. Test sample W2A (magnification 1000x) [Havlik 2012]

Fig. 13 depicts a special compound, which was subsequently identified by metallographic analysis of the cross-section. In addition, longitudinal traces in the direction of the axis of the opening, i.e. in the direction of travel of the roller head [Dugin 2012] [Fiala 2015] [Havlik 2012] [Kouril 2006] [Pokorny 2016].

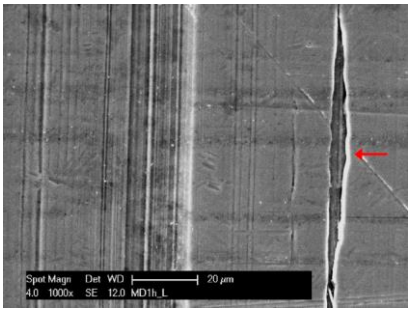

Figure 13. Test sample MD1h (magnification 1000x) [Havlik 2012]

2.8 Microhardness evaluation

To evaluate the deformation of the surface of the machined holes the microhardness of the surface (measured perpendicular to the surface), the microhardness of the base material and the microhardness at two depths beneath the machined surface were measured. Measurement was performed on the Walter Uhl VMHT micro hardness gauge for Vickers hardness measurement [Fiala 2015] [Havlik 2012] [Kouril 2006].

Measurement of the microhardness of the surface of the test sample is schematically indicated in Fig. 14 by imprint No. 1. Measurement of the microhardness of the base material and the microhardness at two depths below the surface in the cross section is schematically indicated in Fig. 14 by imprint No. 2 [Fiala 2015] [Havlik 2012] [Kouril 2006].

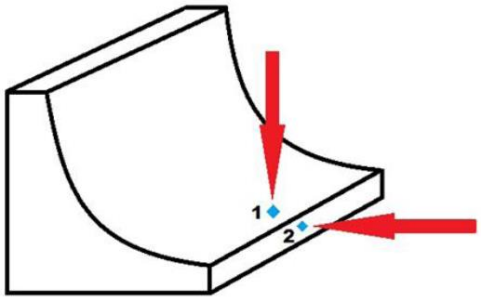

Figure 14. Schematic designation of measured microhardness points on the test sample [Havlik 2012]

Measurement of microhardness of the surface and the base material took place at load F = 3 N. When measuring the microhardness of the surface, three imprints were made on the machined surface, see Table 6 denoted I, II and III, which were evenly spaced throughout the length of the test sample. The measured values of microhardnesses and their mean values are given in Table 6 [Fiala 2015] [Havlik 2012] [Kouril 2006].

Test sample	Microharness HV 0.3			
	I	II	III	Average
MD50	451	472	448	457
W1A	465	458	402	442
W2A	571	656	544	590
MD1h	330	347	342	340

Table 6. Measured microhardness values on the machined surface of the test sample [Havlik 2012]

Measured values in Table 6 shows that a higher value of microhardness HV 0.3 was found for the W2A test sample. This increase could occur as a result of the increased molding and hardening of the surface during machining. Also, a lower value of microhardness was observed in the MD1h test sample. When measuring the microhardness of the base material in cross-section, three imprints were also placed along the entire length of the sample. The measured values of microhardness are shown in Table 7 [Fiala 2015] [Havlik 2012] [Kouril 2006].

Test sample	Microharness HV 0.3			
	I	II	III	Average
MD50	426	426	420	424
W1A	432	458	432	441
W2A	426	420	432	426
MD1h	351	347	334	344

Table 7. Measured values of microhardness of the base material on the surface of the test sample [Havlik 2012]

From the measured values of the microhardness of the base material, see Table 7, again the finding of a significantly lower value for the sample MDh1 is again compared to the other test samples. This difference could be caused by the local heterogeneities resulting from the heat treatment of the blank, see the following metallographic analysis - chap. 2.9 [Fiala 2015] [Havlik 2012] [Kouril 2006].

From the comparison of the results of the micro-hardness measurement HV 0.3 given in Table 6 a Table 7, it has been seen that reinforcement has a reinforcing effect on the surface. For test specimens MD50, W1A and MD1h, reinforcement is negligible. For a W2A test sample, the reinforcement is marked by more than 160 HV 0.3. The reinforcement is even greater than that of the rolled surface when the plastic deformation [Fiala 2015] [Havlik 2012] [Kouril 2006].

2.8.1 Microhardness below the machined surface measured in cross-section

In the transverse direction, the surface (metallographic cut) allowed lower load values, therefore a load value of F = 0.05 N was chosen. Microhardness was measured at depths of 7 µm and 50 µm under the machined surface. The measured values of microhardness at two depths are shown in Table 8 [Fiala 2015] [Havlik 2012] [Kouril 2006].

Test sample	Microharness HV 0.005 in depth 7 µm				Microharness HV 0.005 in depth 50 µm				Differences microharness HV 0.005
	I	II	III	Average	I	II	III	Average	
MD50	523	580	565	556	582	551	523	552	4
W1A	628	684	550	621	498	498	498	498	123
W2A	769	746	769	761	629	612	683	641	120
MD1h	405	475	513	464	387	396	413	399	66

Table 8. Measured microhardness values below the surface of the test sample [Havlik 2012]

From the measured values of microhardness listed in Table 8 it follows that the greatest difference in microhardness - the largest hardening between the immediate proximity of the surface at a depth of 7 µm and the measurement at a depth of 50 µm below the surface, occurred in the test samples W1A and W2A. In both cases, approximately 120 HV 0.005. An approximately half-hardening of the machined surface occurred in the MD1h test sample, which was still rolled after reaming. From Table 8, it is also apparent that a significant increase in the deformation stiffness in the surface of the machined hole has already taken place on the W1A test sample, i.e. using a worn MT3 reaming head in the middle of its life time [Fiala 2015] [Havlik 2012] [Kouril 2006].

2.9 Metallographic analysis of the cross-cut

Metallographic cuttings were made from the test spamples, which were then monitored under the ZEISS A1Z light microscope. The following changes in structure in the form of the hardened layer and the „transgenes“ [Fiala 2015] [Havlik 2012] [Kouril 2006].

The reinforced layer in the MD50 test sample in Fig. 15 has a local occurrence. Its thickness is very variable, it reaches values of up to 5 µm and is characterized by a slightly "banana" shape. The machining tracks in the transverse cross-cut have a sharp progression and a depth of about 0.5 µm [Fiala 2015] [Havlik 2012] [Kouril 2006].

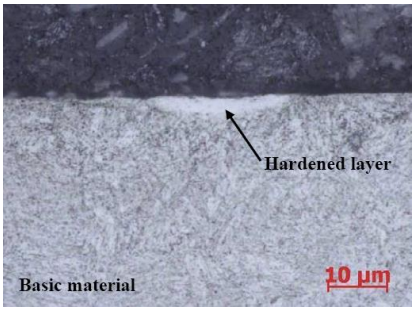

Figure 15. Metallographic cut of the test sample MD50 [Havlik 2012]

The hardened layer of the test sample W1A in Fig. 16 has a continuous character and almost constant thickness of between 1 to 1.8 microns. The grooves in the surface after

machining are smooth and have a shallow depth of 1 µm [Fiala 2015] [Havlik 2012] [Kouril 2006].

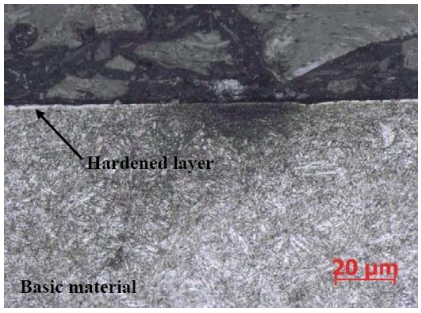

Figure 16. Metallographic cut of the test sample W1A [Havlik 2012]

The hardened layer on the W2A test sample in Fig. 17 has a continuous character. Its thickness is most often between 1 and 1.8 µm, and in some places it is considerably thicker to more than 10 µm. The grooves after machining have a smooth and sharp course and a depth of up to 1 µm [Fiala 2015] [Havlik 2012] [Kouril 2006].

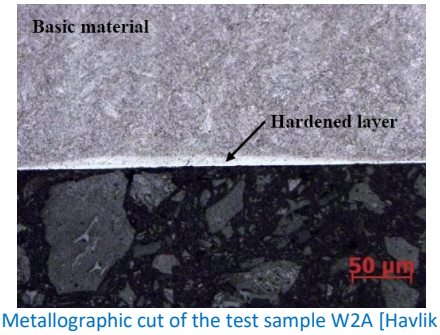

Figure 17. Metallographic cut of the test sample W2A [Havlik 2012]

The hardened layer in the test sample MD1h in Fig. 18 has a local character with a variable thickness of up to 3.5 µm. The grooves after machining have a smooth and sharp course and a depth in the range of 1 to 1.8 µm. The well-known so-called transgenes reaching the depth of up to 3.5 µm have been found in the cut. The presence of these transgenes was also confirmed by observing the surface using a scanning electron microscope. The transgenes were apparently caused by the plunge of the plastically deformed material during the warfare, when a local overlapping occurred in the place of the unevenness - grooves. These transgenes are dangerous because of the possible initiation of fatigue damage, or even the change in the size of the opening during operation [Fiala 2015] [Havlik 2012] [Kouril 2006].

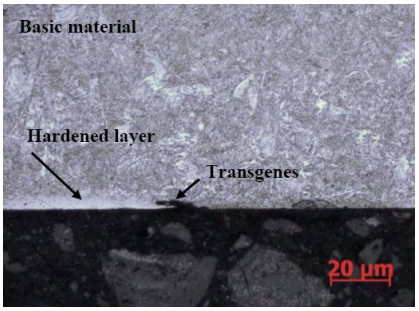

Figure 18. Metallographic cut of the test sample MD1h [Havlik 2012]

3 DISCUSSION

The metallographic analysis also revealed important information about the orientation of sulfide inclusions. In the individual test spamples, their alignment direction was not maintained, indicating that the test pieces were once machined - reamed perpendicularly and once in the longitudinal direction of the main deformation flows in the blank. For test samples MD50, W1A and W2A the sulfides run perpendicularly to the surface, while the sample MD1h (supplied by Sauer Danfoss) is parallel to the machined surface. Additionally, HV 0.3 hardness was determined and a larger metallographic study of the base material of the blank was carried out. When measuring the microhardness, the other test samples made in the experiment had the same hardness in the area of the base material and therefore a test sample was used for comparison MD50 [Fiala 2015] [Fiala 2016] [Havlik 2012] [Kouril 2006] [Kouril 2007].

Fig. 19 shows the direction of forming in a direction transverse to the axis of the recessed aperture (the axis of the opening is horizontal). At the bottom right is a sulfide impression that characterizes the main deformation flow of the material. The structure of the test samples was also oriented W1A a W2A [Fiala 2015] [Fiala 2016] [Havlik 2012] [Kouril 2006] [Kouril 2007].

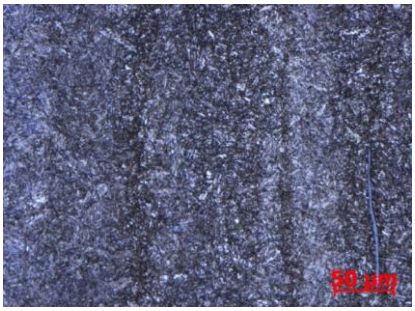

Figure 19. The structure of the base material of the test sample MD50 [Havlik 2012]

A more detailed Fig. 20 shows not only the deformation of the sulfide inclusions but also the bainitic state of the refined structure [Havlik 2012].

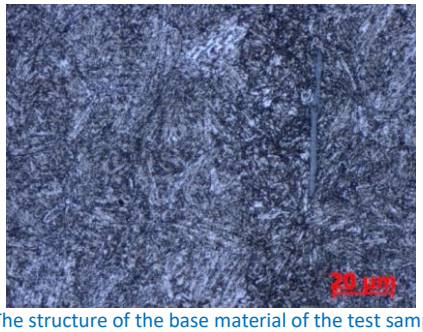

Figure 20. The structure of the base material of the test sample MD50 at greater magnification [Havlik 2012]

At the first view, it is evident from Fig. 21 that the MD1h sample has a different structure. The structure is made up of perlite areas that correspond to the basic state of the 42CrMo4 steel blank. Another difference is the direction of the reamed hole axis, which in this sample is in the direction of the main flow of the formed blank [Fiala 2015] [Fiala 2016] [Havlik 2012] [Kouril 2006] [Kouril 2007].

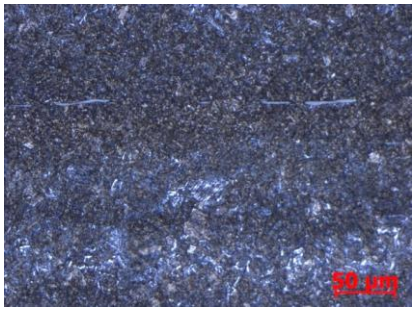

Figure 21. The structure of the base material of the test sample MD1h [Havlik 2012]

A more detailed Fig. 22 confirms the structural difference which consists in imperfect hardening material. The test sample was

too short at austenitizing temperature or, was not hardened at the desired speed. This different structural condition was confirmed by the re-established hardness values of HV 0.3 [Fiala 2015] [Fiala 2016] [Havlik 2012] [Kouril 2006] [Kouril 2007].

In the design of the experiment, it was assumed that the material used for the machining of holes, the 42CrMo4 steel, refined to a strength of 1000 MPa, would be identical to the material of the semifinished material used in the production of Sauer Danfoss hydraulic cylinders. However, the above findings showed that the material of the MD1h sample taken from the cylinder of the hydromotor was not properly hardened, and therefore the testing of the other test samples in the experiment MD50, W1A and W2A took place under different conditions. However, the findings do not affect the comparison of the MD50, W1A and W2A test samples for which conditions were the same. Another difference that may have an effect on the results obtained is the non-corrected direction of machining to the direction of the main deformation of the blank again by comparing the group of test samples MD50, W1A, W2A with the sample MD1h. For these reasons, the results of evaluation of the group of test samples MD50, W1A, W2A can not be compared with the result of evaluation of the test sample MD1h [Fiala 2015] [Fiala 2016] [Havlik 2012] [Kouril 2006] [Kouril 2007].

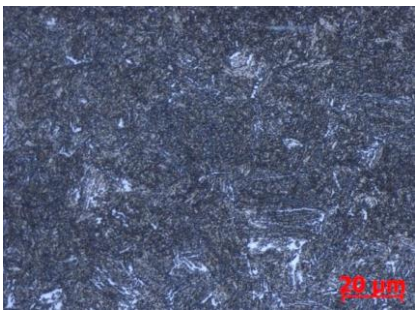

Figure 22. The structure of the base material of the test sample MD1h at greater magnification [Havlik 2012]

4 CONCLUSIONS

High demands on the dimensional and shape accuracy of the produced holes are placed on reamed holes. Another parameter to be observed is the quality of the surface to be machined. The fulfillment of the above requirements is conditioned by the use of high-quality reamers, which are particularly reliable [Fiala 2015] [Fiala 2016] [Havlik 2012] [Kouril 2006] [Kouril 2007].

The analyzes and measurement results in the following conclusions:

- The results of the measurement of the size of the holes showed the expected reduction in the size of the test holes made by the worn MT3 reaming head in the middle of its lifetime - length of the reamed holes L_T = 59,000 mm and test holes made by the worn reaming head MT3 at the end of its lifetime - reamed hole length L_T = 118,000 mm. Specific dimensions for all measured holes ranged from 17.8100 mm to 17.8209 mm.
- The results of circularity and cylindricality showed the lowest values for test holes made by the unused reaming head MT3 at the beginning of its life time. The test holes made with a worn MT3 reaming head in the middle of its life time and at the end of its life time showed an increase in circularity and cylindricality. Specifically, the measured mean circularity values for all test holes ranged from 3.2 µm to 4.4 µm and cylindrical values in the range of 6.0 µm to 8.9 µm.
- The surface roughness measurement results Ra and Rz showed the highest surface roughness values for the test holes made by the unused reaming head MT3 at the beginning of its life time. The test holes made with the worn MT3 reaming head in the middle and at the end of its life time showed lower values. Specifically, the average roughness parameter Ra ranged from 0.1179 µm to 0.1735 µm and the average roughness parameter Rz ranged from 0.7544 µm to 0.9847 µm. From this measurement it is necessary to highlight the highest measured values of surface roughness parameter Ra which reached values below 0.2 µm, which are the values otherwise achieved by the grinding technology. These figures show the current advances in the field of top-of-the-line reaming tools, which today make it possible to replace the abrasive grinding.
- From test holes for further evaluation test samples were taken, which were supplemented by a test sample taken from the cylinder hydraulic motor manufactured in the company Sauer Danfoss. This test was used to evaluate the microhardness, metallographic evaluation, and evaluation of the machined surface under a scanning electron microscope to compare the state of the machined surface to a real hydromotor in practice, followed by roller operations after reaming.
- The results of the microhardness (deformation hardening) measurements showed the reinforcing effect of reaming on the surface of the test holes. The largest hardening was in the test samples, which were made with a worn reaming head MT3 in the middle and at the end of its life time. For these test samles, the microhardness increased in both cases by about 120 HV 0.005. It also follows from the measured values that a significant deformation of the machined test samples occurred with the use of a worn MT3 reaming head in the middle of its life time. A deformation hardening surprisingly found to be about the half of its value was measured at the test sample, taken from the hydromotor, where the deformation hardening was also expected due to the plastic deformation during rolling.
- The results of the metallographic analysis of the cross-cuts of the test samples showed changes in the structure of the surface layer of the test holes. In the test samples from the hole made of the unused reaming head MT3 at the beginning of its life time, the hardened layer was only a local occurrence with a significantly variable thickness of up to 5 µm. Test sample with a hole made of a worn MT3 reamer head in the middle of its life time, the hardened layer had a continuous character and almost constant thickness between 1 µm and 1.8 µm. In the test sample with the hole made of the worn reaming head MT3 at the end of its life time, the hardened layer was again of a continuous character with a thickness of between 1 µm and 1.8 µm, but significantly increased to more than 10 µm in several places. In the test sample taken from the hydromotor, the hardened layer had a local character with a variable thickness of up to 3.5 µm. A well visible so-called „transgenes“; extending to a depth of up to 3.5 µm were also found in the sample

of this test sample. The presence of these transgeneses was also confirmed by observing the surface using a scanning electron microscope.

ACKNOWLEDGMENTS

This article was supported and co-financed from a specific research FSI-S-16-3717 called "Research in Field of Modern Production Technologies for Specific Applications".

REFERENCES

[Bohdan Bolzano, Ltd 2017] Bohdan Bolzano, Ltd Czech Republic. Data Sheets. (in Czech) © 2017, [online]. [seen 2017-03-15]. Available from <http://www.bolzano.cz>

[Dugin 2012] Dugin, A., Popov, A. Effect of the Cutting Tool Wear on the Ploughing Force Values, Manufacturing Technology, 2012, Vol. XVII, No. 1, 2, pp 19-23. ISSN 1211-4162

[Fiala 2015] Fiala, S., Kouril, K., Rehor, J. Modhnology of Finishing of Very Accurate Holes by Reaming and its Influence on Practical Qualities of Products (in Czech), Manufacturing Technology, 2015, Vol. XX, No. 1, pp 17-22. ISSN 1211-4162

[Fiala 2016] Fiala, S., Kouril, K. Cermet Reamers with Chip Formers (in Czech). 2016, pp 116-117, [online]. [seen 2016-09-21]. Available from <http://www.mmspektrum.com/clanek/cermetove-vystruzniky-s-utvareci-trisky.html>

[Forejt 2006] Forejt, M., Piska, M. Theory of Machining, Shaping and Tools (in Czech). Brno: CERM, 2006. ISBN 80-214-2374-9

[Forejt 2010] Forejt, M., Sizova, A., Sedlak, J. Analysis of Modern Grooving Methods using CNC Machines (in Czech). Brno: CERM, 2010. ISBN 978-80-214-4116-3

[Havlik 2012] Havlik, L. Surface Integrity at Reaming with Modern Reaming Head MT3. (in Czech). Brno 2012. Master`s Thesis. Brno University of Technology, Faculty of Mechanical Engineering, Department of Machining Technology. p. 88, 3 appendices. Thesis Supervisor Ing. Karel Kouril, Ph.D.

[Kouril 2006] Kouril, K. Finishing Operations of Reaming (in Czech), MM Industry Spectrum, 2006, Vol. 2006, No. 6, pp 32-33. ISSN 1212-2572

[Kouril 2007] Kouril, K., Fiala, S. Modern Tools for Holes Finishing (in Czech). 2007, pp 42-43, [online]. [seen 2017-03-10]. Available from <www.mmspektrum.com/clanek/moderni-nastroje-pro-dokoncovani-der>

[OE217 – EUREKA] OE217 – EUREKA. Development and Innovation of Tools and Technologies for Finishing of Accurate Holes (in Czech). Brno, 2006. (2006 to 2008, MSM/OE Czech republic). Solver: Stanislav Fiala

[Piska 2010] Piska, M., Slany, M., Madaj, M., Polzer, A. Influence of Process Liquids on Active and Passive Force Elements during Drilling (in Czech). Praha: Czech Engineering Society, 2010. ISBN 978-80-02-02237-4

[Pokorny 2012] Pokorny, Z., Hruby, V., Barborak, O. Characteristics of plasma nitrided Layers in deep Holes, Metallic materials, 2012, Vol. 3, No. 50, pp 209-212. ISSN 0023-432X

[Pokorny 2016] Pokorny, Z., Studeny, Z., Hruby, V. Effect of nitrogen on Surface morphology of layers, Metallic materials, 2016, Vol. 54, No. 2, pp 119-124. ISSN 1338-4252

[Sedlak 2011] Sedlak, J. et al. Evaluation of Feed force Progress during Reaming of holes by MT3 Head and Modelling of its Movement Kinematics (in Czech). Brno, 2011. Brno: Brno University of Technology, Faculty of Machanical Engineering, Department of Machining Technology, p. 32. Final Report about Project Realization: Network to Support Cooperation among Technically and Business Oriented Universities with Companies in South Moravian Region CZ.1.07/2.4.00/12.0017

[Slany 2013] Slany, M. Study of Effects of Passive Force Cutting Elements on Machined Surface (in Czech). Brno 2013. Dissertation Thesis. Brno University of Technology, Faculty of Mechanical Engineering, Department of Machining Technology. p. 137, 1 appendix. Thesis Supervisor prof. Ing. Miroslav Piska, CSc.

[Zouhar 2009] Zouhar, J. Development of Efficient Milling Machines with Use of CAD/CAM and Analysis of Mechanism of Chip Formation (in Czech). Brno 2009. Doctoral Thesis. Brno University of Technology, Faculty of Mechanical Engineering, Department of Machining Technology. p. 104, 7 appendices. Thesis Supervisor doc. Ing. Miroslav Piska, CSc.

CONTACTS:

Assoc. Prof. Josef SEDLAK, Ph.D., MSc.
MSc. Karel KOURIL, Ph.D.
Assoc. Prof. Josef CHLADIL, CSc., MSc.
MSc. Ales JAROS, Ph.D.

Brno University of Technology
Faculty of Mechanical Engineering
Institute of Manufacturing Technology
Department of Machining Technology
Technicka 2896/2, 616 69 Brno, Czech Republic
Phone: +420 541 142 408, sedlak@fme.vutbr.cz,
http://www.fme.vutbr.cz/prdetail.html?pid=16690

Phone: +420 541 142 420, kouril.k@fme.vutbr.cz,
http://www.fme.vutbr.cz/prdetail.html?pid=58840

Phone: +420 541 142 557, chladil@fme.vutbr.cz,
http://www.fme.vutbr.cz/prdetail.html?pid=660

Phone: +420 541 142 404, jaros.a@fme.vutbr.cz,
http://www.fme.vutbr.cz/prdetail.html?pid=76390

Stanislav FIALA

FINAL Tools Inc., Brno
Vlarska 22, 627 00 Brno, Czech Republic
Phone: +420 548 127 314, info@finaltools.cz

MSc. Zdenek FIALA, Ph.D.

Intemac Solutions Ltd., Kurim
Blanenska 1288/27, 664 34 Kurim, Czech Republic
Phone: +420 727 956 438, fiala@intemac.cz